Published in final edited form as:

Nature. 2019 June ; 570(7760): 241–245. doi:10.1038/s41586-019-1257-5.

Cas13-induced cellular dormancy prevents the rise of CRISPR-resistant bacteriophage

Alexander J. Meeske[1,*], **Sandra Nakandakari-Higa**[1], and **Luciano A. Marraffini**[1,2,*]

[1]Laboratory of Bacteriology, The Rockefeller University, 1230 York Ave, New York, NY 10065, USA

[2]Howard Hughes Medical Institute, The Rockefeller University, 1230 York Ave, New York, NY 10065, USA

Abstract

Clustered, regularly interspaced, short palindromic repeat (CRISPR) loci of prokaryotes are composed of 30-40 bp repeats separated by equally short sequences of plasmid and bacteriophage origin known as spacers[1–3]. Spacers are transcribed and processed into short CRISPR RNAs (crRNAs) that are used as guides by CRISPR-associated (Cas) nucleases to recognize and destroy complementary sequences (known as protospacers) within invaders[4,5]. In contrast to most Cas nucleases which destroy the invader's DNA[4–7], the type VI effector nuclease Cas13 employs RNA guides to locate complementary transcripts and catalyze both sequence-specific *cis*-, and non-specific *trans*-RNA cleavage[8]. While it has been hypothesized that Cas13 naturally defends against RNA phages[8], type VI spacer sequences have exclusively been found to match the genomes of double-stranded DNA (dsDNA) phages[9,10], suggesting that Cas13 can provide immunity against these invaders. However, whether and how Cas13 utilizes the *cis*- and/or *trans*-RNA cleavage activities in defending against dsDNA phages is not understood. Here we show that *trans*-cleavage of transcripts halts the growth of the host cell and results in the abortion of the infectious cycle. This depletes the phage population and provides herd immunity to uninfected bacteria. Phages harboring target mutations, which easily evade DNA-targeting CRISPR systems[11–13], are also depleted due to the activation of Cas13 by co-infecting wild type phages. Thus, by acting on the host rather than directly targeting the virus, type VI CRISPR systems not only provide robust defense against DNA phages but also prevent outbreaks of CRISPR-resistant phage.

We investigated the ability of Cas13a to provide phage resistance to *Listeria*, a natural host for the type VI-A CRISPR-Cas system which we previously established as a model to study immunity against plasmid transfer[14]. We constructed *L. ivanovii* ΩCRISPR^{VI}, a strain

*Correspondence to: ameeske@rockefeller.edu, marraffini@rockefeller.edu. **Materials and Correspondence:** ameeske@rockefeller.edu, marraffini@rockefeller.edu.

Author contributions: Experiments were designed by AJM and LAM. AJM conducted spacer library construction and testing, all RNA-sequencing, cell dormancy experiments, phage mutant construction, and escaper cross-protection assays, as well analysis of all NGS data. SN assisted with sequencing the *L. seeligeri* RR4 and *L. ivanovii* RR3 genomes and initial testing of spacers in ϕRR4 immunity. The paper was written by AJM and LAM.

Competing interests: L.A.M. is a cofounder and Scientific Advisory Board member of Intellia Therapeutics, and a co-founder of Eligo Biosciences.

carrying the type VI-A CRISPR locus of *Listeria seeligeri* ATCC35967, which is susceptible to infection by the phage ϕRR4 (Extended Data Fig. 1a–c). To explore Cas13a-mediated phage immunity, we generated a spacer library containing 41,276 unique ϕRR4 sequences, tiled every two nucleotides across both strands of its genome (Supplementary Information 1). We introduced the spacer library into *L. ivanovii* ΩCRISPR^{VI} and infected the cells with ϕRR4. We collected intact cells before and five hours post-infection, and used next-generation sequencing to determine spacer abundance. Wild-type RR3 cells decreased in OD_{600} after infection, but the diverse set of spacers in the library provided protection from lysis (Extended Data Fig. 1d). We calculated enrichment ratios for each spacer as the read count post-infection divided by number of initial reads. The observed enrichment ratios were modest, consistent with previously reported growth defects associated with Cas13a activation[8,14]. As expected from Cas13a's RNA targeting, we found a strong strand bias in spacer efficacy: those generating a crRNA complementary to predicted transcripts (based on ORF direction) displayed substantially higher enrichment ratios than those for which there should not be a target transcript (Fig. 1a–b, Extended Data Fig. 1e, and Supplementary Information 1). To confirm this, we performed RNA-seq analysis of phage-infected cells (Extended Data Fig. 2a) and found a strong correlation between protospacer transcription and the protection conferred by the corresponding spacer (Fig. 1c, Extended Data Fig. 1b and Supplementary Information 1). We selected three individual spacers from the library for further characterization: *spcA*, targeting the ϕRR4 anti-CRISPR region, *spcE*, targeting the early lytic genes, and *spcL*, targeting the late lytic genes (Extended Data Fig. 1a). Each spacer strongly reduced both the efficiency of infective center formation (Fig. 1d) as well as the phage burst size (Fig 1e). Together, these results demonstrate that Cas13a uses crRNAs complementary to phage transcripts to prevent both the establishment and maintenance of infection.

The experiments described above demonstrated that while different individual spacer sequences supported different levels of defense, spacers matching either essential or non-essential transcripts (such as those produced by phage anti-CRISPR genes, see below), and early- or late-expressed RNAs, were capable of mediating a robust defense. This indicates that the function of the target transcript cleaved by Cas13a *cis*-RNase activity does not impact the potency of the type VI-A immune response. To determine the extent of Cas13a-mediated *trans* RNA degradation *in vivo*, we used conventional RNA-seq (Extended Data Fig. 3a) as well as global mapping of RNA 5' ends, a method that detects both the transcription start site (TSS) of primary transcripts as well as the products of Cas13a cleavage. We analyzed both host and phage-derived transcripts in *L. ivanovii* RR3, ΩCRISPR^{VI}(*spcE*) and ΩCRISPR^{VI}(*spcL*) strains after 105 minutes of infection with ϕRR4. In the absence of type VI-A immunity we detected abundant peaks for each TSS over a background signal that is presumably derived from spurious RNA cleavage or alternative transcription initiation (Fig. 2a–d) In contrast, in ΩCRISPR^{VI}(*spcE*) cells we detected extensive cleavage within the ϕRR4 early lytic transcript (Fig. 2a) as well as within host transcripts (Fig. 2c and Extended Data Fig. 3b). Moreover, the average cleavage ratio (defined as the ratio of cleavage products to primary transcript reads) in ΩCRISPR^{VI}(*spcE*) was significantly higher than in RR3 control cells, across all host transcripts (Figs. 2e and Supplementary Information 2). Transcripts of the late lytic operon were undetectable in

ΩCRISPR^{VI}(*spcE*) cells (Fig 2a and Extended Data Fig. 3a) most likely due to the requirement of the products of phage early lytic genes for late gene transcription. Similar results were obtained for ΩCRISPR^{VI}(*spcL*) cells (Figs. 2b, d, f, Extended Data Fig. 3a and Supplementary Information 3). We also detected cleavage of the early lytic transcripts in this strain, presumably a consequence of Cas13a's *trans* RNA degradation. Finally, similar degradation of host RNA was observed in the absence of phage infection, 15 minutes after activation of Cas13a by a chromosomally-encoded target in *L. seeligeri* ATCC35967 (Figs. 3g, h, Extended Data Fig. 3c and Supplementary Information 4). Together, these results indicate that *trans*-RNA cleavage by Cas13a leads to massive degradation of both host and invader RNA *in vivo.*

While DNA-cleaving CRISPR-Cas systems provide immunity through the direct destruction of the phage genome[7,15], we reasoned that the collateral RNA degradation deployed by type VI-A systems might lead to the depletion of host and phage factors required for phage DNA replication; i.e. indirectly support the clearance of the invader's genome. We used qPCR to measure the abundance of phage DNA within RR3 and ΩCRISPR^{VI} strains over the course of ϕRR4 infection (Fig. 3a). Phage DNA failed to accumulate when early-expressed transcripts were targeted by *spcA* and *spcE*, most likely due to the prevention of phage replication mediated by Cas13a's destruction of host and phage transcripts early in the lytic cycle. In contrast, when Cas13a was programmed with *spcL*, phage DNA accumulated to similar levels as the RR3 control. This result indicates that Cas13a can interfere with phage infection at any time during the viral lytic cycle, through a mechanism that does not necessarily prevent the accumulation of phage DNA. We hypothesized that such a mechanism could be based on the growth defect observed during Cas13 targeting of plasmids in both heterologous and native hosts[8,14]. We looked for similar growth defects during phage infection by measuring the optical density (OD_{600}) of *L. ivanovii* RR3 and ΩCRISPR^{VI} cultures after infection. While we detected only mild growth defects at a multiplicity of infection (MOI) of 1 (Extended Data Fig. 4a), at an MOI of 5 CRISPR targeting resulted in a marked growth delay of the cultures (Fig 3b). We and others[8,16] hypothesized that, similarly to abortive infection systems that elicit phage defense in other bacteria[17–19], massive host transcript degradation could result in the dormancy of infected cells and thus prevent viral propagation. To test this, we assessed cell viability and phage titers before and immediately after infection at an MOI of 2, as well as after the first phage burst four hours later (Fig 3c and Extended Data Fig. 4b). Only 10-20 % of RR3 control cells lacking CRISPR remained viable immediately after infection and then suffered a more pronounced loss after 4 hours. In contrast, all three ΩCRISPR^{VI} strains exhibited the same initial viability loss but then recovered at 4 hours, with reduced numbers compared to uninfected control cultures (Fig 3c and Extended Data Fig. 4c). Phage titers mirrored these results, with substantial phage proliferation in RR3 cells during the first four hours of infection, but a significant decrease in phage propagation, even immediately after infection, in cells equipped with type VI-A immunity (Fig. 3d).

These results support a model for Cas13a-mediated immunity in which infected cells stop proliferating and inactivate the phages that invaded them; thus providing passive protection to uninfected cells, which survive and proliferate. Indeed, a viability of 10-20% corresponds to the expected number of uninfected cells at an MOI of 2, which calculated using the

Poisson distribution is 13%. To test this model we first asked whether Cas13a activation elicits cell dormancy. We monitored growth (OD_{600}) after aTc-induction of a target transcript in the native type VI-A host, *L. seeligeri* ATCC35967 (Extended Data Fig 5a). Wild-type (but not ΔCRISPR) cells exhibited growth cessation, with no evidence of lysis. These cultures recovered upon removal of aTc and remained sensitive to re-exposure to the inducer (Extended Data Fig 5b), a result suggesting that the Cas13a-induced dormancy state is reversible. To test this more rigorously, we enumerated viable cells after induction of Cas13a targeting, plating culture samples on solid media without aTc. Over a course of nine hours of target transcription and Cas13a activation, we observed a stable population of viable cells capable of colony formation upon aTc removal (Fig. 3e), demonstrating that cells in which Cas13a was activated cease to grow but do not die. Importantly, these cells were not escape mutants losing CRISPR function, which only accounted for ~1% of the viable population after nine hours (Fig. 3e). Furthermore, Cas13a induction in wild-type, but not in ΔCRISPR cells, provided tolerance to transient exposure to the bactericidal antibiotics ampicillin, ciprofloxacin and streptomycin, which are otherwise lethal to growing cells (Fig. 3f). Finally, to test if cells enter the dormancy state during phage targeting, we took samples of *L. ivanovii* RR3 and ΩCRISPR^{VI} cultures at different times after ϕRR4 infection to enumerate viable cells and determine the vitality of the culture using the reagent resazurin, which is quantitatively converted to fluorescent resorufin by the reducing cytosol of living cells[20]. The CFU values mimicked the results of Fig. 3c above (Extended Data Fig 5c). In contrast, resorufin fluorescence remained constant over the course of the experiment in ΩCRISPR^{VI} cultures (Extended Data Fig 5d), showing that most of the cells of the culture, including those not able to form a colony, stay alive during infection. Altogether, these data demonstrate that, when activated by a target transcript, Cas13a RNase activity promotes a state of cell dormancy, rather than cell death. While dormancy can be reversed by the inhibition of target transcription, it is maintained in infected cells where active phages continue producing protospacer RNA.

Next we investigated whether infected cells could provide herd immunity to uninfected cells in the population, as has been observed for other CRISPR types[12,21,22]. Indeed, we found that phage-sensitive, chloramphenicol-resistant RR3 cells were protected from ϕRR4 infection when co-cultured with ΩCRISPR^{VI}(*spcE*) cells (Fig. 3g). Finally, we directly tested whether the cell dormancy triggered by activation of Cas13a is sufficient to protect against phage infection. We introduced a plasmid harboring a target under an aTc-inducible promoter into *L. ivanovii* ΩCRISPR^{VI}(*spcP*), which carries a spacer that matches the plasmid target, but not any of the phage transcripts. We found that addition of aTc to activate Cas13a before infecting cells with ϕRR4 prevented phage propagation (Fig 3h). Furthermore, we observed a significant survival advantage for the plasmid-targeting strain after 7 hours of ϕRR4 infection (Extended Data Fig. 5e). Together, these results demonstrate that the *trans*-RNA degradation activity of Cas13a is sufficient to provide immunity against dsDNA phages by inducing dormancy in the infected cell, which prevents viral proliferation and protects uninfected cells in the population.

Our observation that plasmid-activated type VI-A CRISPR immunity also protected against infection by a phage not recognized by Cas13a's crRNA guide demonstrates that these systems can provide general, non-specific immunity. This suggests that type VI-A systems

could neutralize “escaper” phages in the population, which contain target mutations that prevent their recognition by the crRNA guide. Such escaper phages easily overcome DNA-targeting CRISPR systems[11–13] but should not be able to successfully infect a host in which a previous infection by a wild-type phage activated Cas13a (a very likely scenario when escapers are rare in the phage population). Indeed, we were not able to detect escaper plaques on lawns of *L. ivanovii* ΩCRISPR^{VI}(*spcE*) or ΩCRISPR^{VI}(*spcA*) cells (Extended Data Fig. 6a–b). To investigate this, we engineered two ϕRR4 mutants that were able to escape *spcA* (ϕRR4^{acr}) and *spcE* (ϕRR4^{early}) targeting (Extended Data Figs. 6a–d). We infected *L. ivanovii* ΩCRISPR^{VI} cells with these mutants and found that their propagation was reduced by 1-2 orders of magnitude when co-infected (1:10^5 ratio) with wild-type ϕRR4 (Fig. 4a–c). Moreover, we obtained similar results when we used the virulent myovirus A511 (ref. [23]), a *Listeria* phage unrelated to ϕRR4, instead of the mutants (Fig. 4a–c). Finally, we tested the prediction that the extent of escaper neutralization should increase with the MOI, as the probability of infection with a wild-type phage also increases. Indeed, cells pre-infected at higher MOIs with wild-type ϕRR4 showed reduced propagation of escaper phages (added at MOI 0.1 to pre-infected cells) (Fig 4d). Adsorption efficiency was unchanged after the first infection, excluding the possibility that competition for phage binding sites prevents the second infection by escaper phages (Extended Data Fig. 6e). Importantly, preinfection of a ΩCRISPR^{II}(*spcE*) strain carrying the type II-A CRISPR system from *Streptococcus pyogenes* programmed with *spcE* with ϕRR4^{acr}, which lacks the anti-CRISPR genes that inhibit Cas9 cleavage (Extended Data Fig. 6c, f) did not prevent either the Cas9-escaper ϕRR4$^{acr\text{-}esc}$ or A511 from avoiding Cas9 targeting. Therefore, cross-protection is a feature of Cas13a targeting, and not a ϕRR4-specific phenomenon, such as superinfection exclusion. Together, these data indicate that type VI-A immunity against wild-type ϕRR4 cross-protects against infection by both protospacer escape mutant phages and other unrelated viruses. Thus, by acting on the infected host rather than directly on the target phage, Cas13a activation leads to broad and nonspecific immunity against dsDNA phages.

Here we show that during the type VI-A CRISPR-Cas response against dsDNA phages, the RNase Cas13a performs crRNA-guided recognition of phage RNA, resulting in massive degradation of host and phage transcripts. Although it is possible that this degradation interferes with the phage lytic cycle to contribute to the overall defense, we believe that the fundamental feature of type VI-A immunity is the dormancy of the host cell produced by the destruction of host transcripts. This is similar to other phage defense strategies known as abortive infection[24]. We postulate that in the absence of a mechanism to specifically destroy the phage DNA, target transcription continues, Cas13a remains active and the host cells neither resume growth nor lyse. Therefore, the infected cell can continue to adsorb phages, abort their infectious cycle and eliminate them from the culture.

To date, all the other studied CRISPR types possess DNA cleavage activities capable of destroying the infecting phage genome[6,7,15,25,26]. Therefore immunity is achieved by a direct attack on the invader, followed by the survival of the infected cells. A consequence of direct interference with the phage lytic cycle is that mutant escapers can overcome targeting, kill the infected cell and propagate. In contrast, during type VI-A CRISPR-Cas immunity, the small fraction of escaper phages present in the viral population most likely end up

infecting a cell in which Cas13a was previously activated by a wild-type, target-bearing phage, and are therefore also neutralized. Phage density, escaper frequency, and spacer targeting efficiency are all variables likely to affect the extent of this cross-protection mechanism.

Instead of employing abortive infection to limit the propagation of escaper phages, the DNA-degrading CRISPR systems usually acquire new spacer sequences that can target other regions of the phage[12]. Given the negative selection suffered by cells in which type VI-A immunity is triggered, and the strong protection against escapers provided by Cas13a, it is unclear how spacer acquisition might operate in these systems. One possibility is that spacers are acquired from the injected genomes of defective phage particles that fail to activate their transcriptional program[27]. Alternatively, phage genomes could occasionally be cleared from the cell after Cas13a activation, permitting the cell to recover from dormancy. If such a mechanism exists, the infected cell itself would benefit from the presence of the type VI CRISPR system and immunity would not be an exclusively altruistic event.

Methods

Data availability

The *L. seeligeri* RR4 and *L. ivanovii* RR3 genome sequences, along with raw reads from the spacer library deep sequencing, paired end RNA-seq, and 5’ end mapping have been deposited in the Sequence Read Archive under BioProject accession number PRJNA512236. Lists of strains, plasmids, and oligonucleotides used in this study are available in Supplementary Information 5.

Code availability

Custom scripts used in analysis of spacer library data as well as RNA 5’ end mapping data are available upon request..

Bacterial strains and growth conditions

The type VI CRISPR system was derived from *L. seeligeri* ATCC strain 35967 (Rocourt and Grimont). *L. seeligeri* RR4 and *L. ivanovii* RR3 were obtained from Jean-Paul Lemaître (INRA, Dijon, France). All *Listeria* strains were propagated in Brain Heart Infusion (BHI) broth or agar at 30°C. Unless otherwise stated, plasmids were cloned in *E. coli* DH5α, miniprepped, and transformed into the conjugative donor strain *E. coli* SM10 for conjugative mating. All *E. coli* strains were cultured in Lysogeny Broth (LB) at 37°C.

Phage isolation and propagation

Isolation of ϕRR4 was carried out by overnight induction of *L. seeligeri* RR4 at OD 0.1 using mitomycin C at 2 μg/mL. The induced culture supernatant was diluted to single plaques on a lawn of *L. ivanovii*, and a single plaque was purified twice to ensure homogeneity. To generate high-titer phage lysates, 50 mL of *L. ivanovii* culture was infected with ϕRR4 at MOI 0.1, OD 0.1 and the infection proceeded overnight. The lysate was filtered and concentrated to 1 mL using Amicon Ultra 100MWCO columns.

Infective center and burst size quantitation

L. ivanovii strains were grown to mid-exponential phase, and 0.6 mL of culture at OD600 0.5 was infected with ϕRR4 or derivatives at an MOI of 0.1. Adsorption was carried out for 5 min, followed by three washes with 1 mL BHI to remove unbound phage, and the samples were resuspended to a final volume of 1 mL. Infective centers were enumerated by titering PFU on a lawn of naïve *L. ivanovii* RR3 at the initial time point. Burst size was calculated by dividing the PFU after the first burst by the starting PFU.

E. coli – L. seeligeri conjugation

Donor *E. coli* SM10 or β2163 Δ*dapA* strains carrying *E. coli-Listeria* shuttle vectors were cultured in LB containing 100 μg/mL ampicillin (for pAM8-derived vectors) or 25 μg/mL chloramphenicol (for pPL2e-derived vectors). Recipient *L. seeligeri* or *L. ivanovii* strains were cultured in BHI. 100 μL each of saturated donor and recipient cultures were combined in 10 mL BHI, and concentrated onto a 0.45 μm membrane filter, which was then overlaid onto a BHI agar plate containing 8 μg/ml oxacillin, which weakens the cell wall, enhancing conjugation. Mating plates were incubated for 4 hr at 37°C, then cells were resuspended in 2 mL BHI and plated at 30°C on selective BHI media containing 50 μg/mL nalidixic acid (which kills donor *E. coli* but not recipient *Listeria*). Selection for plasmid recipients was performed with either 15 μg/mL chloramphenicol (for pAM8-derived vectors) or 1 μg/mL erythromycin (for pPL2e-derived vectors).

Cloning of CRISPR locus and spacer library construction

The *L. seeligeri* type VI CRISPR locus was introduced to *L. ivanovii* RR3 by cloning into the PSA site-specific integrating vector pPL2e[28] via three-piece Gibson assembly using (1) a synthetic gene fragment containing the native promoter and CRISPR array modified to contain only two repeats and BsaI sites for spacer cloning (amplified with oAM462/127), (2) the *cas13a* gene (amplified with oAM463/94), and (3) BamHI-SalI digested pPL2e, resulting in the plasmid pAM125. Cloning of individual spacers was carried out by ligation of annealed oligos into BsaI-digested pAM125. For spacer library construction, a library of 41,276 × 85 nt oligonucleotides, each containing a unique ϕRR4-matching spacer, repeat homology, BsaI sites, and universal priming sites oligonucleotides was purchased from Twist Biosciences. The library was made double-stranded by PCR and the product was purified by phenol-chloroform extraction. Spacers were introduced into pAM125 via Golden Gate cloning with BsaI-HFv2 (New England Biolabs) and T7 DNA ligase, then electroporated into Endura Duo electrocompetent cells. 400,000 colonies were pooled, the plasmids isolated, and electroporated into the conjugative donor strain β2163 Δ*dapA* in the presence of 1.2 mM diaminopimelic acid (DAP). Conjugation into *L. ivanovii* was carried out as described above, except for the presence of 1.2 mM DAP during mating. Transconjugants were isolated in the presence of erythromycin (to select for ΩCRISPR^{VI} integration) and the absence of DAP to prevent growth of the auxotrophic donor *E. coli.* The ΩCRISPR^{II} strain was constructed by cloning the type II-A CRISPR-Cas9 system from *Streptococcus pyogenes* into the *E. coli-Listeria* shuttle vector pAM8 [14]. A single spacer was retained with two SapI sites for spacer cloning (pAM307). Cloning of individual spacers was carried out by ligation of annealed oligos into SapI-digested pAM307. A pAM307 variant

carrying ϕRR4 *spcE* (pAM325) was conjugated into *L. ivanovii*, selecting on media containing 50 μg/mL nalidixic acid and 15 μg/mL chloramphenicol to generate ΩCRISPR^{II}.

Gene deletions and replacements in *Listeria*

Allelic replacement in *L. seeligeri* or *L. ivanovii* was conducted as previously described [14]. Briefly, 1 kb homologous sequences flanking each side of the region to be replaced were cloned into pAM215, a suicide plasmid unable to replicate in *Listeria,* that also carries a *lacZ* and chloramphenicol resistance (*cat*) markers. This plasmid was transferred to *Listeria* strains via conjugation as described above, and 100 μL of resuspended cells was plated for selection on 50 μg/mL nalidixic acid and 15 μg/mL chloramphenicol. Isolated transconjugants (integrants) were streak-purified and confirmed *lacZ*+ by patching on BHI plates containing 100 μg/mL 5-Bromo-4-Chloro-3-Indolyl β-D-Galactopyranoside (X-gal). Integrants were passaged (grown to saturation, then diluted 1000 fold) 3-4 times in BHI without selection. Passaged cultures were diluted and plated on BHI X-gal, and incubated 2-3 days at 37°C. White (*lacZ*-) colonies (excisants) were isolated, confirmed chloramphenicol-sensitive, and checked for the deletion by PCR using primers flanking the desired deletion followed by Sanger sequencing.

Bacterial genome sequencing and assembly

Chromosomal DNA was prepared from 2 mL cultures of *L. seeligeri* RR4 and *L. ivanovii* RR3 via lysozyme treatment and phenol-chloroform extraction and ethanol precipitation. DNA samples were sheared using a Covaris sonicator, prepared for deep sequencing using the Illumina TruSeq Nano DNA LT kit, and paired-end 2×300 bp sequencing was conducted on the MiSeq platform. Reads were quality-trimmed using Sickle (https://github.com/najoshi/sickle), and assembled into contigs using Abyss (https://github.com/bcgsc/abyss). Finally, contigs were mapped to reference *L. seeligeri* and *L. ivanovii* genomes using Medusa (http://combo.dbe.unifi.it/medusa). Automated genome annotation was performed using BaSys (https://www.basys.ca). Raw reads as well as assembled genomes have been deposited to GenBank under BioProject accession number PRJNA512236.

Spacer selection, deep sequencing, and analysis

The spacer library was grown to OD 0.3 and a pre-infection sample was harvested. The remaining culture was infected with ϕRR4 at an MOI of 1, and surviving cells were harvested five hours later. Chromosomal DNA was prepared from both samples, and the CRISPR array was amplified using oAM459/16. Library preparation from the resulting PCR products was conducted using the Illumina TruSeq Nano DNA LT kit, followed by 150 bp single-end sequencing using the MiSeq platform. Spacer sequences flanked by perfect repeats were extracted and mapped to the ϕRR4 genome using bowtie2. Reads at each position in the genome were calculated and normalized to total spacer reads, and the enrichment ratio for a given spacer was calculated as the read count post-infection divided by that pre-infection. Spacers with fewer than 10 reads pre-infection were discarded to reduce noise (26,766 spacers retained). Raw sequencing reads for each time point have been deposited under BioProject accession number PRJNA512236.

RNA sequencing

To isolate RNA from *Listeria*, the equivalent of 3 mL culture at OD_{600} 0.5 was pelleted, and lysed by 3 min treatment with 2 mg/mL lysozyme followed by the addition of sarkosyl at 1%. A fixed amount of *S. aureus* RNA was added to each sample immediately after lysis for global RNA normalization. RNA was purified from these lysates using the Zymo Direct-Zol RNA miniprep plus kit according to the manufacturer's instructions. Genomic DNA was eliminated using the Ambion Turbo DNase-free kit. Ribosomal RNA was depleted using the Illumina Ribo-Zero rRNA removal (Bacteria) kit. After rRNA removal, libraries were prepared for deep sequencing using the TruSeq Stranded mRNA Library prep kit, skipping mRNA purification and beginning at the RNA fragmentation step. Paired-end (2×75bp) sequencing was performed on the NextSeq platform. Paired-end sequencing data for phage-infected *L. ivanovii* RR3, ΩCRISPR^{VI}(*spcE*), and ΩCRISPR^{VI}(*spcL*) strains, as well as aTc-treated *L. seeligeri* wild-type (Ptet-*spc4*) and ΔCRISPR (Ptet-*spc4*) have been deposited under BioProject accession number PRJNA512236.

For 5' end mapping, RNA was first purified, DNase-treated and rRNA depleted as above, then concentrated using the Zymo RNA Clean & Concentrator 5 kit and 5' phosphorylated with T4 polynucleotide kinase (NEB). 5' triphosphates were removed using *E. coli* polyphosphatase, and a 5' RNA adapter was added using T4 RNA Ligase. The library was fragmented using Agilent RNA fragmentation reagents, and reverse transcribed using SuperScript IV with an adapter primer ending in nine randomized nucleotides. The resulting cDNA libraries were amplified by PCR and purified using AMPure beads, then single end 150 bp sequencing was carried out on the MiSeq platform. 5' end sequencing data for phage-infected *L. ivanovii* RR3, ΩCRISPR^{VI}(*spcE*), and ΩCRISPR^{VI}(*spcL*) strains, as well as aTc-treated *L. seeligeri* wild-type (Ptet-*spc4*) and ΔCRISPR (Ptet-*spc4*) have been deposited under BioProject accession number PRJNA512236.

RNA-seq analysis

RNA-seq reads were mapped to the corresponding genome using bowtie2. Coverage was calculated at each genome position, normalized to the total number of *S. aureus* reads (representing the spike-in), and the ratio of CRISPR+:CRISPR- reads was calculated. If zero reads were detected, a pseudocount was added. For RNA 5' end mapping analysis, reads were mapped as above, with only the 5' end position tabulated. Operonic transcripts were manually annotated from the paired-end transcriptomic data, and these boundaries were used to calculate the fraction of reads mapping within or outside the transcriptional start site (TSS). The site within 500 nucleotides upstream of the start codon containing the most 5' reads in WT cells was designated as the TSS. Reads mapping within 5 nucleotides of this site were counted as TSS reads. For transcripts in which at least 20 reads were detected in each sample, the cleavage ratio was calculated as the read count downstream of the TSS divided by that within the TSS. Normalization to the TSS accounts for differences in gene expression generated by pleiotropic effects such as the degradation of transcription factor mRNAs. This cleavage ratio also allowed us to capture events in which Cas13a-mediated degradation did not produce stable cleavage products. Tables are provided showing cleavage ratios for each transcript in phage-infected *L. ivanovii* RR3 and ΩCRISPR^{VI}(*spcE*) (Supplementary Information 2), ΩCRISPR^{VI}(*spcL*) (Supplementary Information 3), as well

as aTc-treated *L. seeligeri* wild-type (Ptet-*spc4*) and ΔCRISPR (Ptet-*spc4*) (Supplementary Information 4).

ϕRR4 escaper mutant construction

ϕRR4 mutants were generated by allelic exchange using the integration of the suicide vector pAM215 into the *L. seeligeri* RR4 lysogen as described above. Mutant prophage were confirmed by PCR and sequencing, and induced with mitomycin C as described above.

Herd immunity experiment

L. ivanovii RR3 cells carrying a *cat* gene encoding resistance to chloramphenicol were co-cultured at a 1:1 ratio with either wild type RR3 or ΩCRISPR^{VI}(*spcE*) cells, then the population was infected with ϕRR4 at OD_{600}=0.1, MOI 1, for 7h at 30°C. Viable chloramphenicol-resistant cells were enumerated prior to and 7h after infection.

Immunity by plasmid targeting

L. ivanovii ΩCRISPR^{VI}(*spcP*) cells were transformed with pAM211 (empty-vector) or pAM212 (aTc-inducible *spcP* target) via conjugative mating. Cells carrying each plasmid and the CRISPR locus were grown to OD_{600}=0.1, and exposed to 100 ng/mL aTc was added for 1h. Then, cells were infected with ϕRR4 at MOI 1 for 7h at 30°. Viable CFU were enumerated prior to and after infection. Alternatively, the efficiency of ϕRR4 infective center formation was measured on cells 1h post-aTc treatment.

Cell vitality assay

Cell vitality was measured with the resazurin-based cell vitality reagent alamarBlue HS (ThermoFisher) according to the manufacturer's instructions. Briefly, 100ul of cell culture was mixed with 10ul of alamarBlue HS, incubated for 20 min while shaking at 37 °C, and fluorescence (excitation: 560 nm, emission: 590 nm) was measured on a Tecan Infinite M200 Pro plate reader with monochromator module with a fixed gain setting of 79. Uninfected cells in the same media as all experimental samples were used as live cell standards, and the same samples heated for 5 min at 95 °C were used as dead cell standards. 10% and 50% live cell mixture standards were made to assess accuracy of vitality measurements. Dead cell signal was subtracted as background from all resorufin signal values. Resorufin signal values for all samples were normalized to values pre-infection.

Phage co-infection plaque assays

For phage co-infection assays to assess the efficiency of escaper infection in the presence and absence of co-infecting wild-type phage, escaper phage stocks were diluted to approximately 5×10^4 PFU/mL in BHI medium, then mixed with BHI containing either no phage or 5×10^9 PFU/mL wild-type ϕRR4. Serial 10-fold dilutions of phage mixtures were made and 2 μl of each dilution was spotted onto BHI top agar lawns seeded with 100 μl of saturated cultures of ΩCRISPR^{VI} strains. ϕRR4^{acr} escaper mixtures were spotted on ΩCRISPR^{VI}(*spcA*) lawns, while ϕRR4^{early} escaper mixtures were spotted on ΩCRISPR^{VI}(*spcE*) lawns. A511 mixtures were spotted on both targeting lawns. Co-infections comparing Cas9 and Cas13 were conducted the same way, except ϕRR4^{acr} was

used as the activating phage, and was mixed in 10^5-fold excess with ϕRR4$^{acr\text{-}esc}$ or with A511. Mixtures were spotted onto BHI top agar lawns seeded with 100 μl of saturated ΩCRISPR^{VI}(*spcE*) or ΩCRISPR^{II}(*spcE*) culture.

Extended Data

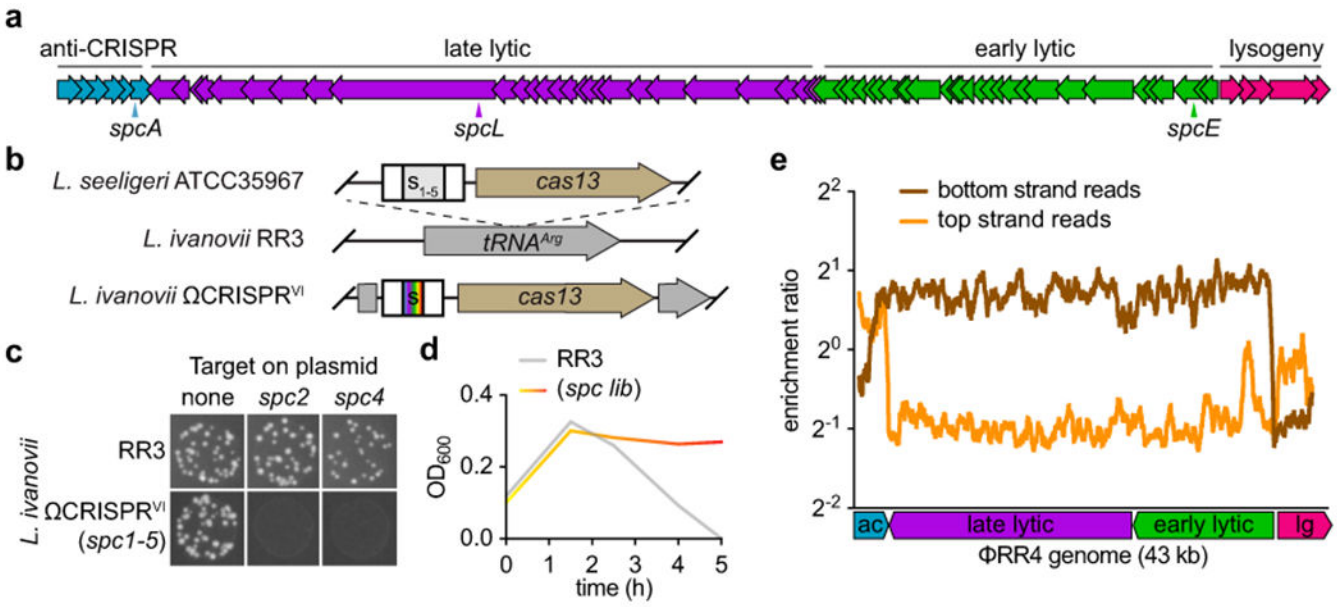

Extended Data Fig. 1. *Listeria* phage infection model for studying type VI-A CRISPR immunity.

(**a**) Diagram of the ϕRR4 genome, with individual genes depicted within the anti-CRISPR, early lytic, late lytic, and lysogenic regions. *Listeria seeligeri* ATCC35967 harbors a five-spacer type VI-A CRISPR locus[29], but phages infecting this strain have not yet been identified. We sequenced the genome of *L. seeligeri* RR4[30] and found it contains a 42 kb prophage, ϕRR4, that is similar to the A118 listeriophage[31]. Although ϕRR4 particles induced from the lysogen did not infect *L. seeligeri* ATCC35967, ϕRR4 propagated in the closely related *Listeria ivanovii* RR3 strain (99.2% 16S rRNA identity)[30]. (**b**) The type VI-A CRISPR locus of *L. seeligeri* ATCC35967 was inserted into the *tRNA*^{Arg} gene of *Listeria ivanovii* RR3 using the vector pAM125, generating *L. ivanovii* ΩCRISPR^{VI}. Different strains with either the five spacers naturally present in this system (*spc1-5*), individual spacers matching the genome of ϕRR4 (*spcA*, *spcE*, *spcL*), or a ϕRR4 spacer library (*spc lib*), were generated. For the latter, 41,276 ϕRR4-matching spacers were selected, tiled every 2 nt across the phage genome, with both strands equally represented. (**c**) Test of type VI-A anti-plasmid immunity in *L. ivanovii* ΩCRISPR^{VI}(*spc1-5*). Plasmids with *spc2* or *spc4* targets in the chloramphenicol resistance cassette were conjugated into *L. ivanovii* RR3 or ΩCRISPR^{VI}(*spc1-5*) and transconjugants selected on nalidixic acid and chlorampehnicol. Transconjugants receiving an empty vector lacking a target sequence are shown as a negative control. Example is representative of two biological replicates. (**d**) Prevention of ϕRR4 lytic infection by the type VI spacer library. Spacer library cells (yellow-orange gradient) or cells lacking CRISPR (gray) were infected with ϕRR4 at OD_{600} = 0.1, MOI=1 and OD_{600} was monitored over time. Example is representative of two biological replicates. (**e**) 100 bp sliding window average spacer enrichment ratio (spacer abundance post-infection / pre-infection) for spacers targeting top (orange) and bottom (brown) strands.

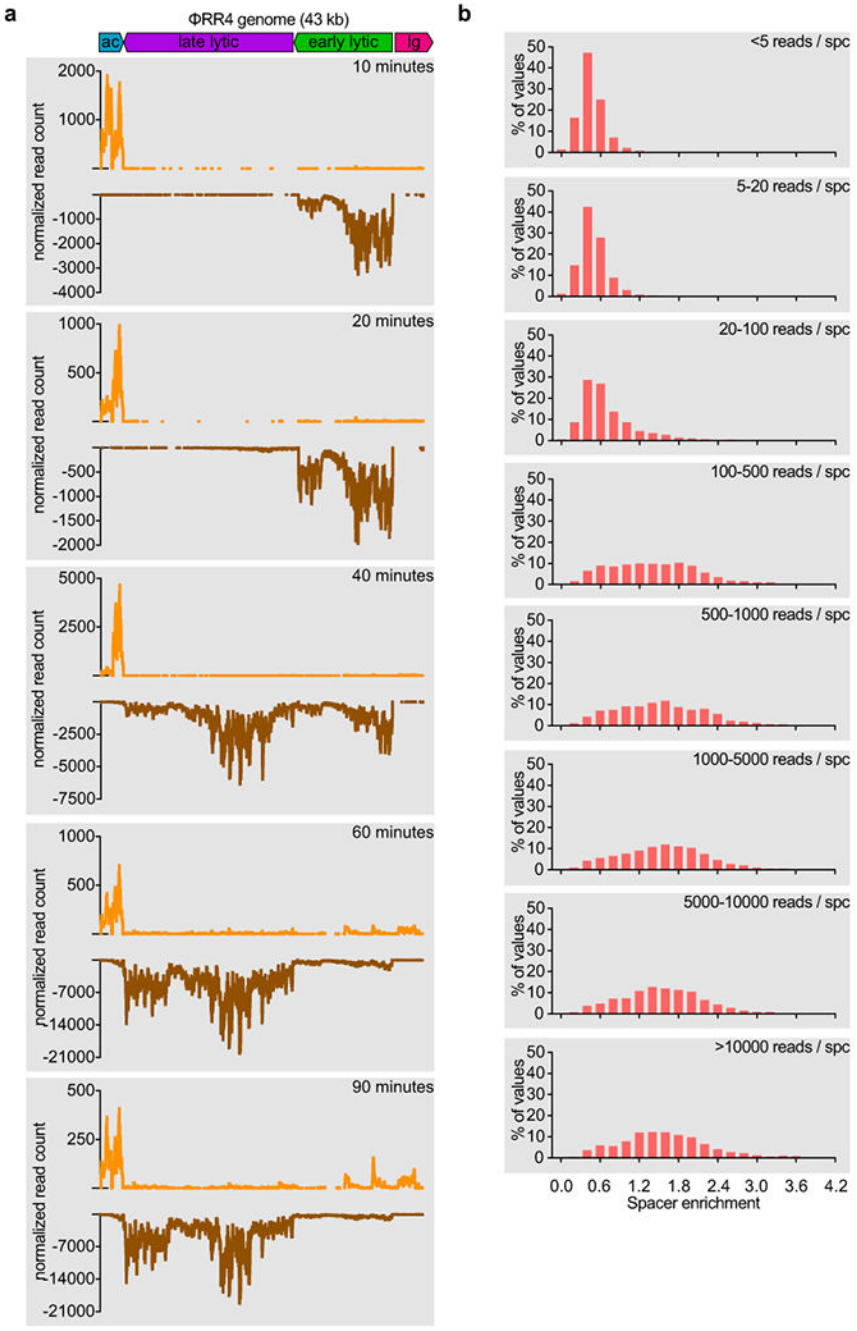

Extended Data Fig. 2. ϕRR4 transcriptome and enrichment of corresponding targeting spacers.

(**a**) RNA-seq over the course of ϕRR4 infection. Wild-type *L. ivanovii* RR3 was infected with ϕRR4 at MOI 1 and samples were harvested for transcriptomic analysis by paired-end RNA-seq at the indicated time points. Reads were mapped to the ϕRR4 genome and normalized to the total reads per sample. Top strand mapped reads are shown in orange, bottom strand in brown. Examples are representative of two biological replicates. (**b**) Spacer enrichment correlates with target transcription, with no additional protection conferred above a critical expression threshold. Spacer abundance in the library was assessed pre-

infection as well as 5 hours post-infection with ϕRR4 at MOI 1. Spacer enrichment distributions are shown, with individual histograms representing different tiers of target transcript abundance for the corresponding protospacer.

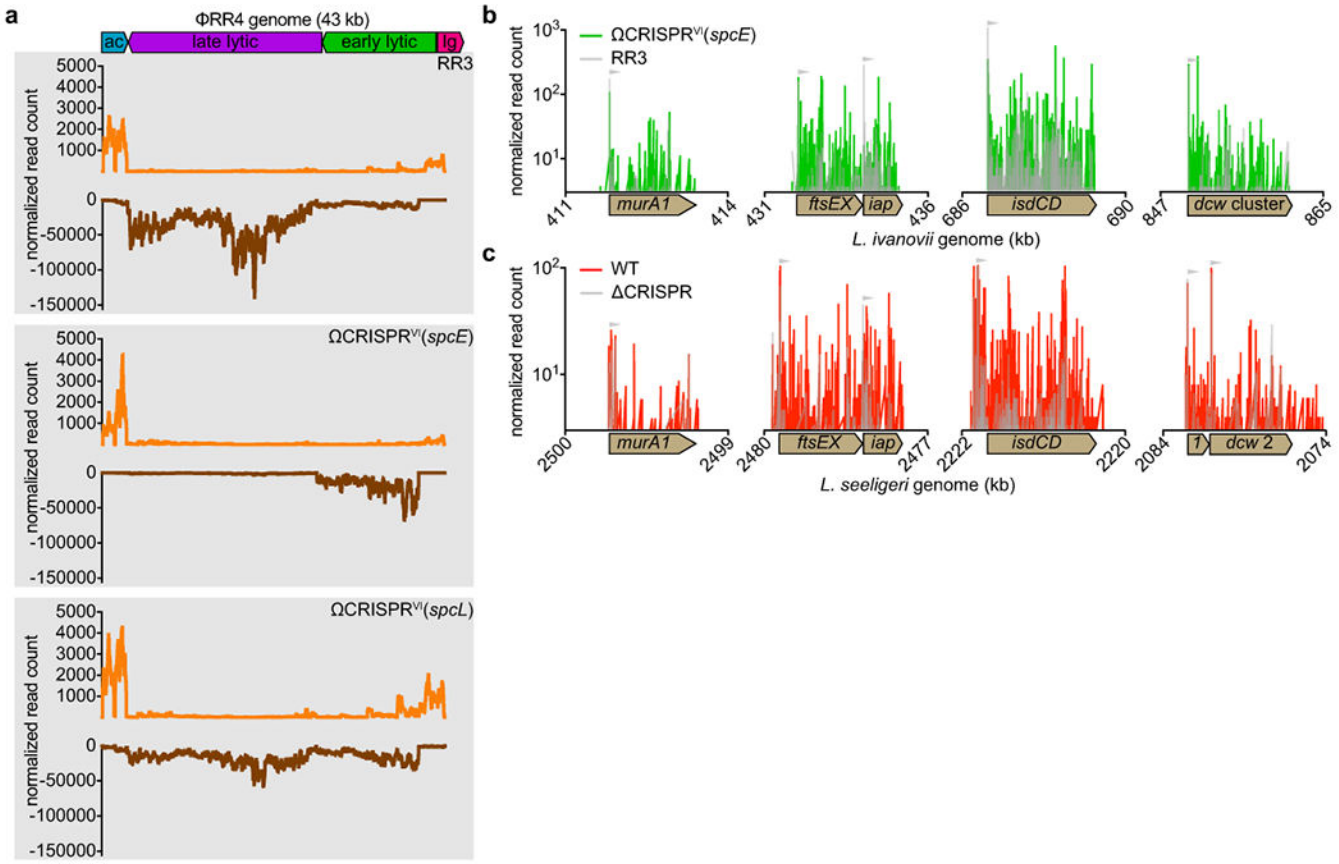

Extended Data Fig. 3. Cas13a-mediated cleavage of phage and host transcripts detected by RNA-seq.

(**a**) Abundance of phage transcripts assessed by conventional paired-end RNA-seq 1.75 hours post infection with ϕRR4 in *L. ivanovii* RR3 wild-type, ΩCRISPR^{VI}(*spcE*) or ΩCRISPR^{VI}(*spcL*) strains. Reads were mapped to the ϕRR4 genome and normalized to the abundance of a spike-in RNA, with top strand reads shown in orange and bottom strand reads in brown. Both ΩCRISPR^{VI}(*spcE*) and ΩCRISPR^{VI}(*spcL*) targeting result in elevated early transcript cleavage products (see Fig. 2a–b) and the reduction of late transcript abundance. Examples are representative of two biological replicates. (**b**) *L. ivanovii* host mRNA cleavage detected by 5’ end mapping in *L. ivanovii* RR3 wild-type (gray) and ΩCRISPR^{VI}(*spcE*) (green) strains 1.75 hours post infection with ϕRR4. The height of each peak represents the detected abundance of the corresponding mRNA 5’ end, with transcriptional start sites depicted as gray arrows. Four regions of the genome are depicted: *murA1*, *ftsEX*/*iap*, *isdCD*, division and cell wall (*dcw*) cluster. Abundant intragenic cleavage products are generated in the ΩCRISPR^{VI}(*spcE*) strain. Examples are representative of two biological replicates. (**c**) The four corresponding genomic regions in (**b**) shown for the native type VI CRISPR host *L. seeligeri*, wild type (red) and ΔCRISPR (gray), 15 minutes after aTc-induction of a target transcript. The *dcw* cluster is broken into two operons in *L. seeligeri.* Examples are representative of two biological replicates.

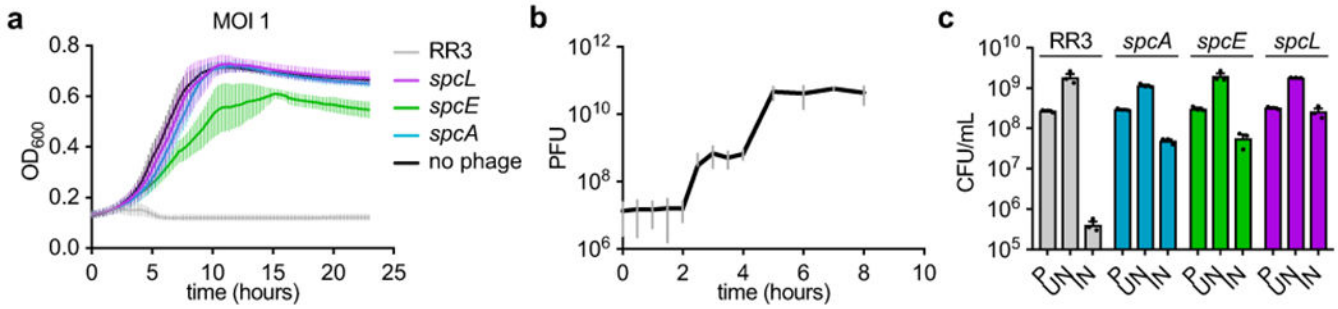

Extended Data Fig. 4. *Trans*-RNase activity is sufficient to limit growth of both ϕRR4 phage and ΩCRISPR^{IV} host.

(**a**) *L. ivanovii* RR3, ΩCRISPR^{VI}(*spcA, spcE,* or *spcL*) strains at OD_{600}=0.05 were infected with ϕRR4 at MOI 1 and growth was monitored over 24 hours. Each curve represents the mean of three biological replicates ±s.e.m. (**b**) Quantitation of ϕRR4 infective centers over time on wild-type *L. ivanovii* RR3. Cells were infected with ϕRR4 at MOI 0.1 and allowed to adsorb 5 minutes, then cells were washed 3 times to remove free phage. Infective centers were counted every 30 minutes by enumerating plaque-forming units on a lawn of phage-susceptible RR3 cells. Each data point represents the mean of three biological replicates ±s.e.m. (**c**) Survival of the indicated strains during ϕRR4 infection at MOI 2. CFU were titered pre-infection (P) and 4 hours post-infection (IN) or mock-infection (UN). Each bar represents the mean of three biological replicates ±s.e.m.

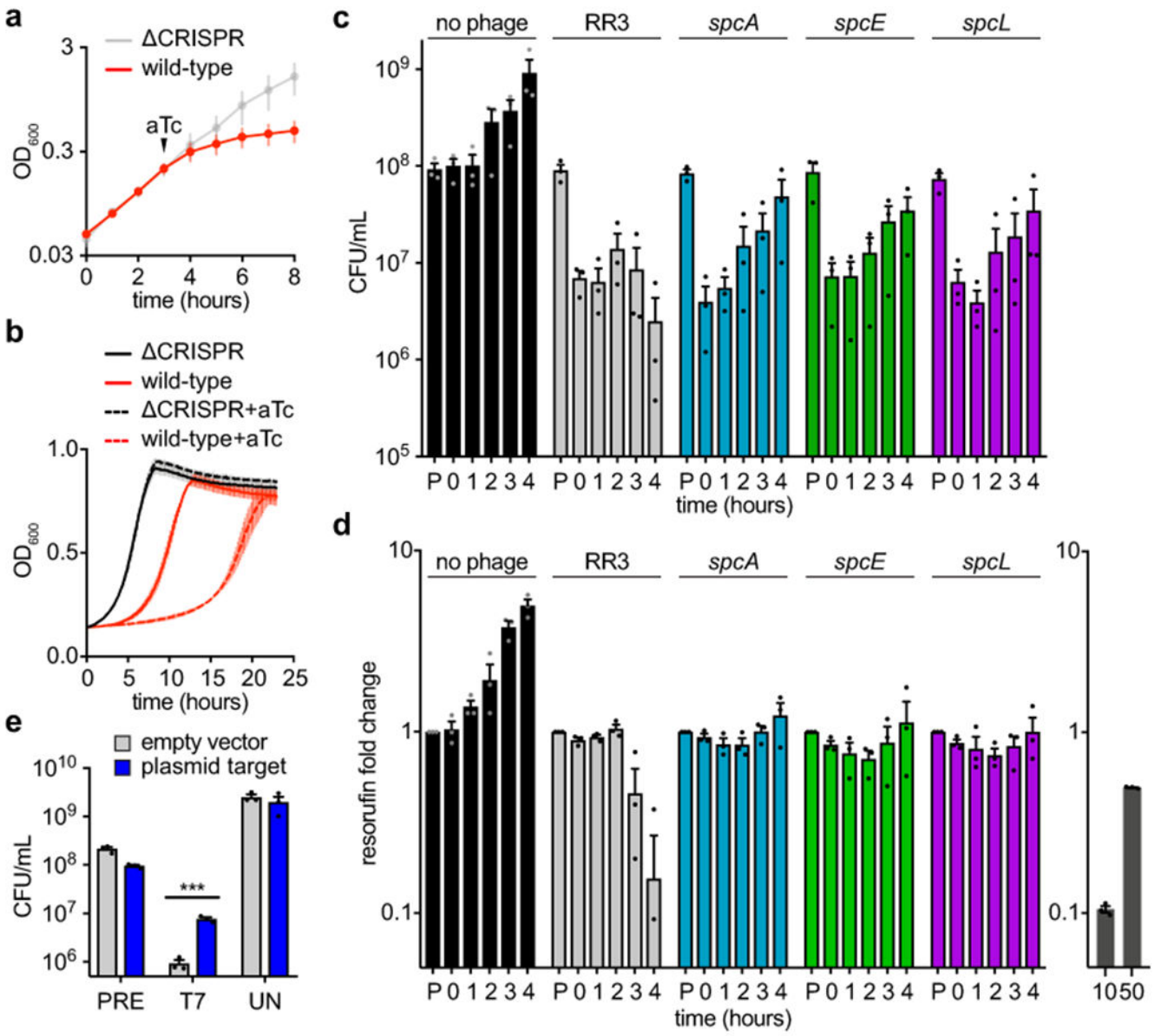

Extended Data Fig. 5. Cas13a activation induces reversible dormancy of the host.

(**a**) Growth arrest (measured as the culture OD_{600}) induced by target transcription in wild-type *L. seeligeri* (but not the ΔCRISPR mutant) harboring an aTc-inducible protospacer RNA. Arrow indicates time of 100 ng/mL aTc addition. Each data point represents the mean of three biological replicates ±s.e.m. (**b**) Wild-type and ΔCRISPR *L. seeligeri* cultures carrying an aTc-inducible target transcript were exposed to 100 ng/mL aTc for 3 hours as in (**a**), then diluted (at time 0 hours) to OD_{600}=0.05 in fresh media in the presence or absence of aTc, and growth was monitored over 24 hours. Each curve represents the mean of three biological replicates ±s.e.m. (**c**) Immediate reduction in CFU upon phage infection of *L. ivanovii* RR3 or ΩCRISPR^{VI} strains. The indicated strains were infected with ϕRR4 at MOI 2, and CFU titers in the infected cultures were monitored over time. Pre-infection (P) and mock-infection titers were also measured. Each bar represents the mean of three biological

replicates ±s.e.m. (**d**) Cell vitality within ΩCRISPR^{VI} cultures during phage infection. Cell vitality was measured in samples of cultures from (**c**) by monitoring conversion of nonfluorescent resazurin to fluorescent resorufin at each time point. Resorufin signal from heat-killed cells was subtracted from all samples as background, and each signal was normalized to pre-infection value. 10% and 50% live cell standards (mixed with heat-killed cells) are shown to demonstrate quantitative capability of vitality assay. Each bar represents the mean of three biological replicates ±s.e.m. (**e**) Phage-susceptible *L. ivanovii* ΩCRISPR^{VI}(*spcP*) cells harboring a spacer against an aTc-inducible plasmid target RNA (or empty vector control) were treated with aTc for 1h to pre-activate Cas13a, then infected with ϕRR4 at MOI 1. Viable CFU were enumerated pre-infection (PRE), 7 hours post-infection (T7) or mock-infection (UN). *** indicates a significant difference, determined by two-sided Student's t-test, p=0.0005. Each bar represents the mean of three biological replicates ±s.e.m.

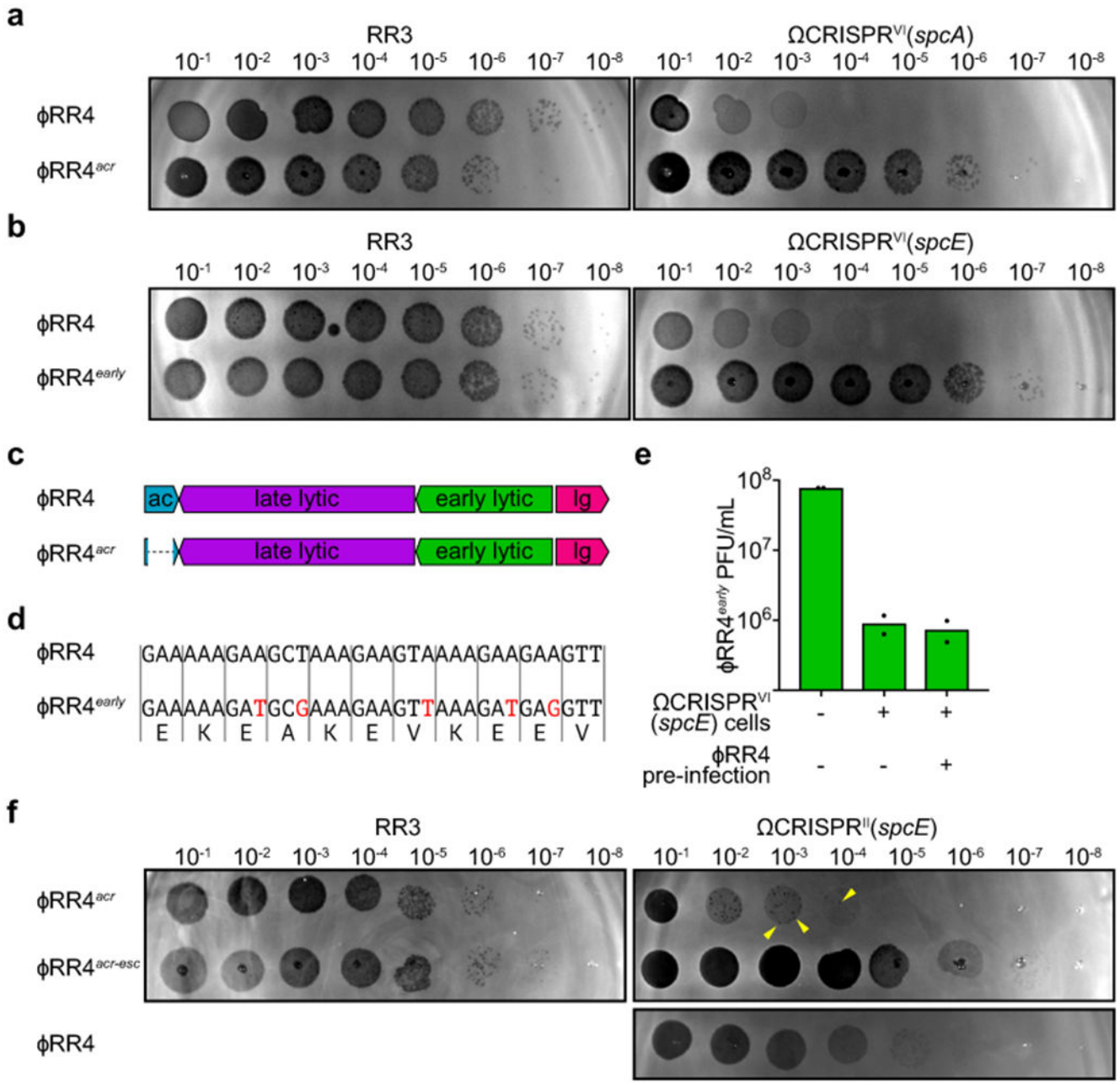

Extended Data Fig. 6. Absence of CRISPR-resistant escape mutants and validation of engineered escaper phage.

(**a**) Efficiency of plaquing assays with wild-type ϕRR4 and engineered *spcA*-escaper phage ϕRR4^{acr} infecting *L. ivanovii* RR3 and ΩCRISPR^{VI}(*spcA*) strains. Phages were diluted and spotted onto top agar lawns containing the indicated strain. Escaper plaques are not observed in the presence of type VI CRISPR targeting. The ϕRR4^{acr} mutant, lacking the *acr* region targeted by *spcA*, is viable and evades CRISPR targeting. Examples are representative of two biological replicates. (**b**) Same as (**a**) but testing *spcE*-escaper phage ϕRR4^{early} and the ΩCRISPR^{VI}(*spcE*) strain. Examples are representative of two biological replicates. (**c**) Design of the ϕRR4^{acr} mutant, harboring a deletion of the putative anti-CRISPR genes of

ϕRR4 (**d**) Design of ϕRR4^{early} mutant, depicting wild-type and mutant *spcE* target sequence. (**e**) Cells pre-infected with wild-type ϕRR4 continue to adsorb escaper phage 2 hours after infection. ΩCRISPR^{VI}(*spcE*) cells were infected with wild-type ϕRR4 at MOI 5 for 2 hours (an uninfected control is shown for comparison), then washed three times with fresh medium to remove free phages. ϕRR4^{early} was added to cells (or to a cell-free control) at MOI 0.1 for 5 minutes, cells and bound phage were pelleted, and free phage in the supernatant were enumerated as PFU formed on a lawn of ΩCRISPR^{VI}(*spcE*) cells. Mean PFU are shown from two biological replicates (**f**) Efficiency of plaquing assay using RR3 and ΩCRISPR^{II}(*spcE*) strains. we generated a ΩCRISPR^{II}(*spcE*) strain carrying the type II-A CRISPR system from *Streptococcus pyogenes* programmed with *spcE* against ϕRR4. This strain has very limited immunity to wild-type ϕRR4, but is highly immune to the ϕRR4^{acr} mutant, which lacks anti-CRISPR-Cas9 genes. Cas9-resistant ϕRR4^{acr} escaper plaques are evident in plaque assay and highlighted with yellow carets. One escaper, ϕRR4$^{acr\text{-}esc}$, was isolated and confirmed resistant to Cas9 targeting. Examples are representative of two biological replicates.

Supplementary Material

Refer to Web version on PubMed Central for supplementary material.

Acknowledgments:

We thank all members of the Marraffini lab for advice and encouragement, A. Varble for helpful discussion, and J.T. Rostøl for a critical reading of the manuscript. *L. seeligeri* RR4 and *L. ivanovii* RR3 were generous gifts from Jean-Paul Lemaître (INRA, Dijon, France). Support for this work comes from the National Institute of Health Director's Pioneer Award 1DP1GM128184-01 (to LAM). LAM is an investigator of the Howard Hughes Medical Institute. AJM is a Helen Hay Whitney postdoctoral fellow.

References:

1. Mojica FJ, Diez-Villasenor C, Garcia-Martinez J & Soria E Intervening sequences of regularly spaced prokaryotic repeats derive from foreign genetic elements. J. Mol. Evol. 60, 174–182, (2005). [PubMed: 15791728]
2. Bolotin A, Quinquis B, Sorokin A & Ehrlich SD Clustered regularly interspaced short palindrome repeats (CRISPRs) have spacers of extrachromosomal origin. Microbiology 151, 2551–2561, (2005). [PubMed: 16079334]
3. Pourcel C, Salvignol G & Vergnaud G CRISPR elements in *Yersinia pestis* acquire new repeats by preferential uptake of bacteriophage DNA, and provide additional tools for evolutionary studies. Microbiology 151, 653–663, (2005). [PubMed: 15758212]
4. Barrangou R et al. CRISPR provides acquired resistance against viruses in prokaryotes. Science 315, 1709–1712, (2007). [PubMed: 17379808]
5. Brouns SJ et al. Small CRISPR RNAs guide antiviral defense in prokaryotes. Science 321, 960–964, (2008). [PubMed: 18703739]
6. Marraffini LA & Sontheimer EJ CRISPR interference limits horizontal gene transfer in staphylococci by targeting DNA. Science 322, 1843–1845, (2008). [PubMed: 19095942]
7. Garneau JE et al. The CRISPR/Cas bacterial immune system cleaves bacteriophage and plasmid DNA. Nature 468, 67–71, (2010). [PubMed: 21048762]
8. Abudayyeh OO et al. C2c2 is a single-component programmable RNA-guided RNA-targeting CRISPR effector. Science 353, aaf5573, (2016). [PubMed: 27256883]

9. Smargon AA et al. Cas13b Is a Type VI-B CRISPR-Associated RNA-Guided RNase Differentially Regulated by Accessory Proteins Csx27 and Csx28. Mol. Cell 65, 618–630 e617, (2017). [PubMed: 28065598]

10. Yan WX et al. Cas13d Is a Compact RNA-Targeting Type VI CRISPR Effector Positively Modulated by a WYL-Domain-Containing Accessory Protein. Mol. Cell 70, 327–339 e325, (2018). [PubMed: 29551514]

11. Deveau H et al. Phage response to CRISPR-encoded resistance in *Streptococcus thermophilus*. J. Bacteriol. 190, 1390–1400, (2008). [PubMed: 18065545]

12. van Houte S et al. The diversity-generating benefits of a prokaryotic adaptive immune system. Nature 532, 385–388, (2016). [PubMed: 27074511]

13. Pyenson NC, Gayvert K, Varble A, Elemento O & Marraffini LA Broad Targeting Specificity during Bacterial Type III CRISPR-Cas Immunity Constrains Viral Escape. Cell Host Microbe 22, 343–353 e343, (2017). [PubMed: 28826839]

14. Meeske AJ & Marraffini LA RNA Guide Complementarity Prevents Self-Targeting in Type VI CRISPR Systems. Mol. Cell 71, 791–801 e793, (2018). [PubMed: 30122537]

15. Westra ER et al. CRISPR immunity relies on the consecutive binding and degradation of negatively supercoiled invader DNA by Cascade and Cas3. Mol. Cell 46, 595–605, (2012). [PubMed: 22521689]

16. Koonin EV & Zhang F Coupling immunity and programmed cell suicide in prokaryotes: Life-or-death choices. Bioessays 39, 1–9, (2017).

17. Parreira R, Ehrlich SD & Chopin MC Dramatic decay of phage transcripts in lactococcal cells carrying the abortive infection determinant AbiB. Mol. Microbiol. 19, 221–230, (1996). [PubMed: 8825768]

18. Fineran PC et al. The phage abortive infection system, ToxIN, functions as a protein-RNA toxin-antitoxin pair. Proc Natl Acad Sci U S A 106, 894–899, (2009). [PubMed: 19124776]

19. Short FL et al. Selectivity and self-assembly in the control of a bacterial toxin by an antitoxic noncoding RNA pseudoknot. Proc Natl Acad Sci U S A 110, E241–249, (2013). [PubMed: 23267117]

20. Shiloh MU, Ruan J & Nathan C Evaluation of bacterial survival and phagocyte function with a fluorescence-based microplate assay. Infect. Immun. 65, 3193–3198, (1997). [PubMed: 9234774]

21. Watson BNJ, Staals RHJ & Fineran PC CRISPR-Cas-Mediated Phage Resistance Enhances Horizontal Gene Transfer by Transduction. *MBio* 9, (2018).

22. Payne P, Geyrhofer L, Barton NH & Bollback JP CRISPR-based herd immunity can limit phage epidemics in bacterial populations. Elife 7, (2018).

23. Klumpp J et al. The terminally redundant, nonpermuted genome of Listeria bacteriophage A511: a model for the SPO1-like myoviruses of gram-positive bacteria. J. Bacteriol. 190, 5753–5765, (2008). [PubMed: 18567664]

24. Rostol JT & Marraffini L (Ph)ighting Phages: How Bacteria Resist Their Parasites. Cell Host Microbe 25, 184–194, (2019). [PubMed: 30763533]

25. Yan WX et al. Functionally diverse type V CRISPR-Cas systems. Science, (2018).

26. Zetsche B et al. Cpf1 is a single RNA-guided endonuclease of a class 2 CRISPR-Cas system. Cell 163, 759–771, (2015). [PubMed: 26422227]

27. Hynes AP, Villion M & Moineau S Adaptation in bacterial CRISPR-Cas immunity can be driven by defective phages. Nat Commun 5, 4399, (2014). [PubMed: 25056268]

Online references

28. Lauer P, Chow MY, Loessner MJ, Portnoy DA & Calendar R Construction, characterization, and use of two Listeria monocytogenes site-specific phage integration vectors. J. Bacteriol. 184, 4177–4186, (2002). [PubMed: 12107135]

29. Rocourt J, Schrettenbrunner A, Hof H & Espaze EP [New species of the genus Listeria: Listeria seeligeri]. Pathol Biol (Paris) 35, 1075–1080, (1987). [PubMed: 3313216]

30. Lemaitre JP, Duroux A, Pimpie R, Duez JM & Milat ML Listeria phage and phage tail induction triggered by components of bacterial growth media (phosphate, LiCl, nalidixic acid, and acriflavine). Appl. Environ. Microbiol. 81, 2117–2124, (2015). [PubMed: 25595760]

31. Loessner MJ, Inman RB, Lauer P & Calendar R Complete nucleotide sequence, molecular analysis and genome structure of bacteriophage A118 of Listeria monocytogenes: implications for phage evolution. Mol. Microbiol. 35, 324–340, (2000). [PubMed: 10652093]

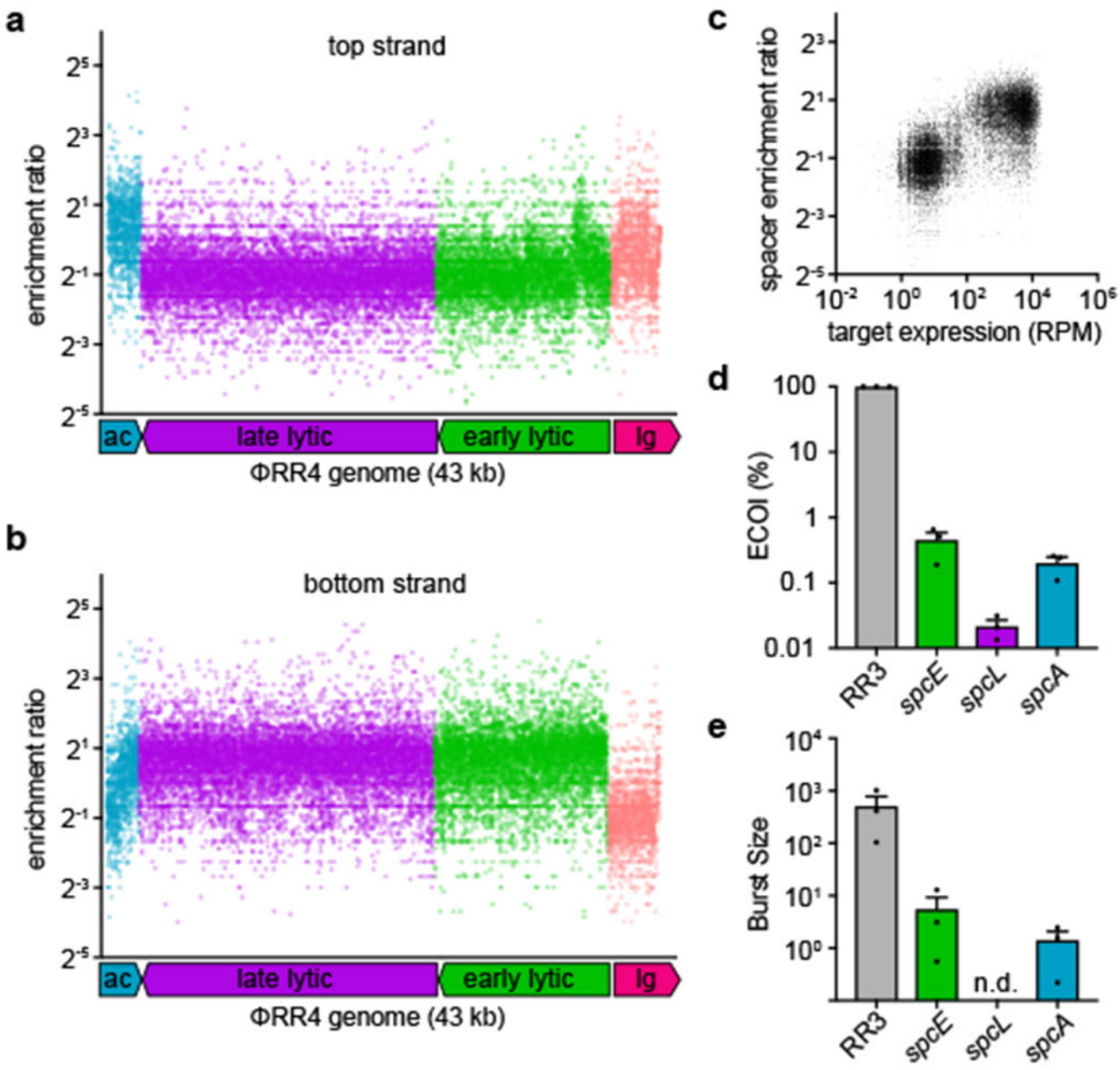

Fig. 1. Cas13a DNA phage infection upon protospacer transcription.

(**a**-**b**) Enrichment of spacers targeting the top (**a**) or bottom (**b**) strands of the ϕRR4 genome after phage exposure, plotted by position. (**c**) Correlation of target transcript expression (measured in reads per million mapped reads, RPM) and enrichment of the corresponding spacer. (**d**) Mean (±s.e.m.) efficiency of ϕRR4 infective center formation (n=3 biological replicates) on strains lacking CRISPR (RR3) or ΩCRISPR^{VI} strains programmed with a *spcE*, *spcL*, or *spcA*. (**e**) Mean (±s.e.m.) ϕRR4 burst size for the strains tested in (**d**) (n=3 biological replicates); n.d., not detectable.

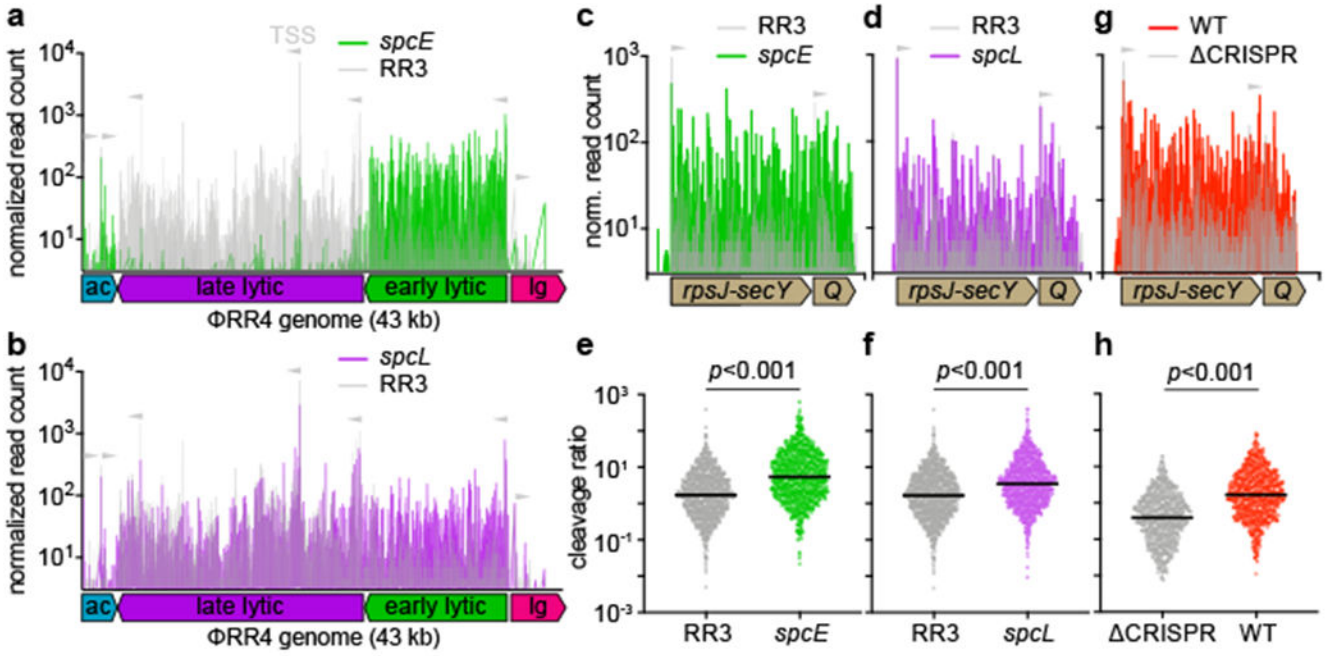

Fig. 2. Cas13a elicits widespread cleavage of host and phage transcripts.

(**a**-**d**) RNA 5' end mapping of ϕRR4 (**a**, **b**) or *rpsJ-secY-rplQ* (**c**, **d**) transcripts after infection of *L. ivanovii* RR3 or ΩCRISPR^{VI} programmed with *spcE* (**a**, **c**) or *spcL* (**b**, **d**) strains. Putative transcriptional start sites (TSS) are depicted with gray arrows. Representative of two biological replicates. (**e**) Global analysis of host transcript cleavage by Cas13a during the). Cleavage ratio (black bar, mean value) for every host transcript in the experiment shown in (**c**) (n=1027 transcripts, unpaired two-sided Student's *t*-test). (**f**) Same as (**e**) but for the experiment shown in (**d**), (n=1092 transcripts). (**g**) Same as (**c**) but for *L. seeligeri* wild-type and ΔCRISPR strains after addition of aTc to induce target transcription. (**h**) Same as (**e**) but for the experiment shown in (**g**), (n=862 transcripts).

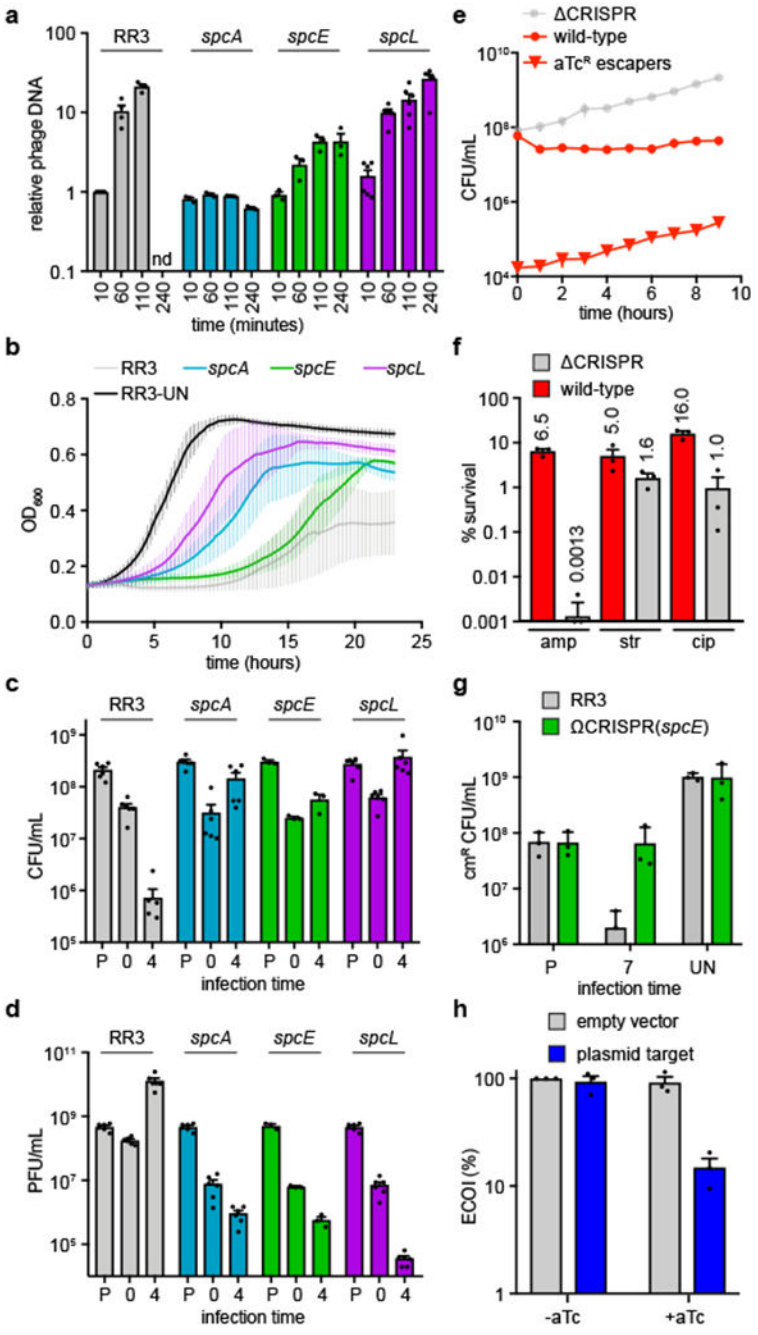

Fig. 3. Cas13a-induced cell dormancy is sufficient to abort lytic infection and limit phage propagation.

(**a**) Mean (±s.e.m., n=3 biological replicates) phage DNA content after infection of *L. ivanovii* RR3 and ΩCRISPR^{VI}(*spcA, spcE,* or *spcL*) strains with ϕRR4 at MOI 1, normalized to value for RR3 cells at 10 minutes post-infection. (**b**) Mean (±s.e.m., n=3 biological replicates) OD_{600} values of *L. ivanovii* RR3 and ΩCRISPR^{VI}(*spcA, spcE,* or *spcL*) cultures after infection with ϕRR4 at MOI 5. Uninfected RR3 is also shown (RR3-UN). (**c**) Mean (±s.e.m., n=6 biological replicates) CFU (colony-forming units) present in *L.*

ivanovii RR3 and ΩCRISPR^{VI}(*spcA, spcE* or *spcL*) cultures prior to (P), immediately after (0), and 4 hours post-infection with ϕRR4 at MOI 2. (**d**) Same as (**c**) but measuring PFU titer. (**e**) Mean (±s.e.m., n=3 biological replicates) CFU from *L. seeligeri* wild-type and ΔCRISPR cultures after transcription of a chromosomal target and plating on media lacking aTc. Escaper mutants in the wild-type culture were counted on plates with aTc. (**f**) Mean (±s.e.m., n=3 biological replicates) survival of *L. seeligeri* wild-type and ΔCRISPR cultures in the presence of ampicillin, streptomycin or ciprofloxacin after activation of Cas13. (**g**) Mean (±s.e.m., n=3 biological replicates) chloramphenicol-resistant CFU/ml before (P), 7 hours after (7) and without (UN) infection with ϕRR4 at MOI 1 of a 1:1 mix of phage-susceptible, chloramphenicol-resistant (cm^{R}) *L. ivanovii* RR3 and chloramphenicol-sensitive *L. ivanovii* RR3 or ΩCRISPR^{VI}(*spcE*). (**h**) Mean (±s.e.m., n=3 biological replicates) efficiency of center of infection (ECOI) after addition of ϕRR4 to phage-susceptible *L. ivanovii* ΩCRISPR^{VI}(*spcP*) cells harboring a plasmid an aTc-inducible *spcP* target or an empty vector control.

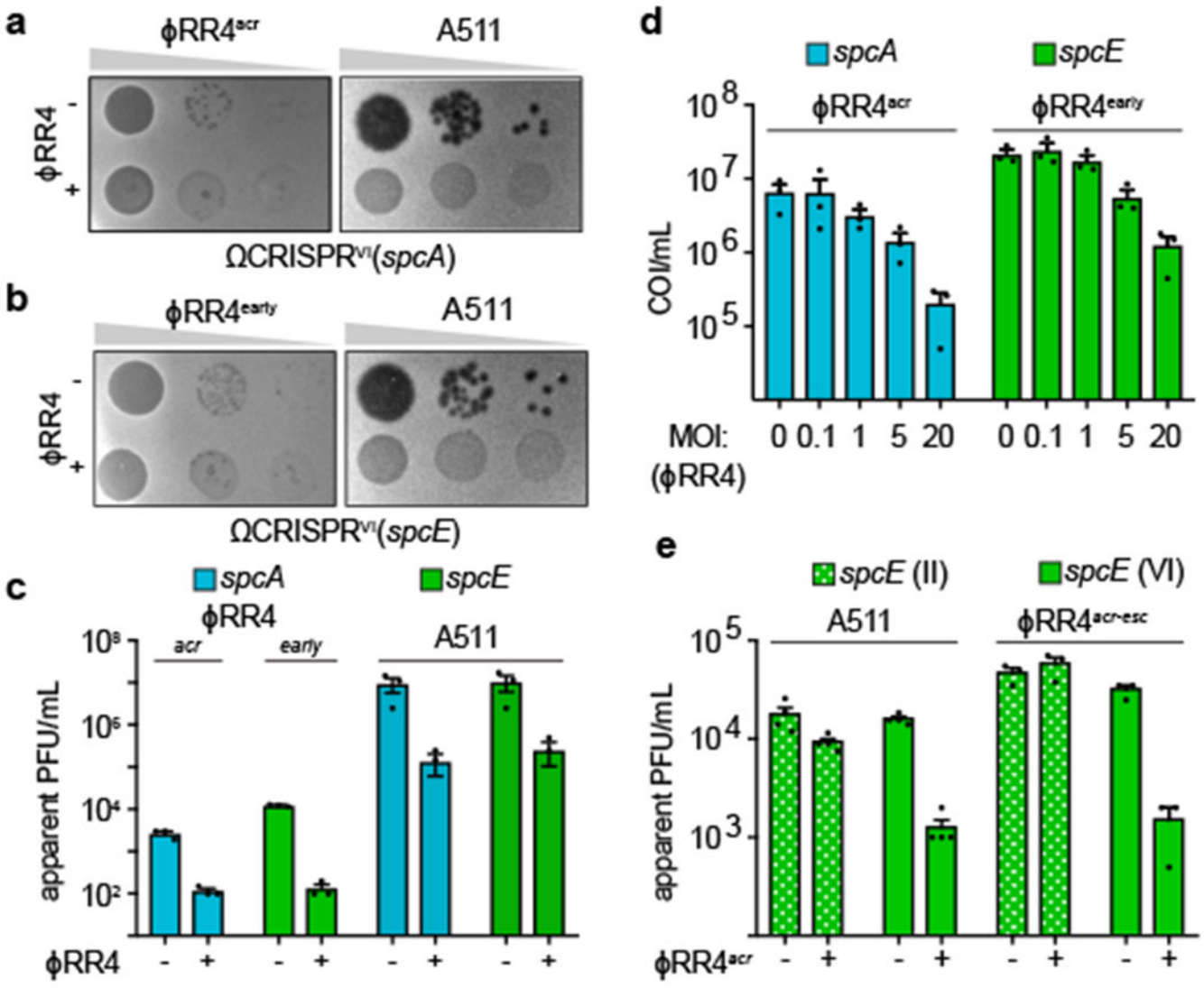

Fig. 4. Cas13a activation suppresses viral escape by providing immunity against untargeted phage.

(**a**) ϕRR4^{acr} (*spcA*-escaper) or A511 were diluted in the presence or the absence of 10^5-fold excess wild-type ϕRR4, and plated on *L. ivanovii* ΩCRISPR^{VI}(*spcA*) lawns. Examples are representative of 3 biological replicates. (**b**) Same as (**a**), but using a ΩCRISPR^{VI}(*spcE*) strain and the *spcE*-escaper ϕRR4^{early}. (**c**) Mean (±s.e.m., n=3 biological replicates) PFU titers obtained in panels (**a**-**b**). (**d**) Mean (±s.e.m., n=3 biological replicates) center of infection (COI) titer of ϕRR4^{acr} and ϕRR4^{early} escaper phages after infection at MOI 0.1 of ΩCRISPR^{VI}(*spcA*) and ΩCRISPR^{VI}(*spcE*) cells, respectively, that were pre-infected for 2 hours with wild-type ϕRR4 at the indicated MOIs. (**e**) Mean (±s.e.m., n=3 biological replicates) plaquing efficiency for A511 and ϕRR4$^{acr\text{-}esc}$ phages on ΩCRISPR^{II}(*spcE*) or ΩCRISPR^{VI}(*spcE*) cells, in the presence and absence of excess ϕRR4^{acr}.